

R. LONGTIN<sup>1,2,✉</sup> \*  
C. FAUTEUX<sup>1,2</sup>  
E. CORONEL<sup>3</sup>  
U. WIKLUND<sup>3</sup>  
J. PEGNA<sup>2</sup>  
M. BOMAN<sup>1</sup>

# Nanoindentation of carbon microfibers deposited by laser-assisted chemical vapor deposition

<sup>1</sup> Department of Materials Chemistry, The Ångström Laboratory, Uppsala University, Box 538, 75121 Uppsala, Sweden  
<sup>2</sup> Freeform Fabrication Laboratories, Department of Mechanical Engineering, École Polytechnique de Montréal, Box 6079, Station A, Montréal, PQ H3C 3A7, Canada  
<sup>3</sup> Department of Materials Science, The Ångström Laboratory, Uppsala University, Box 534, 75121 Uppsala, Sweden

Received: 15 September 2003/Accepted: 27 October 2003  
Published online: 21 January 2004 • © Springer-Verlag 2004

**ABSTRACT** Carbon microfibers were deposited using laser-assisted chemical vapor deposition at atmospheric and sub-atmospheric pressures. Precursor pressures and incident laser powers were varied. Fibers were cast in acrylic resin and polished to allow nanoindentation of the cross sections. Cross-sectional roughness was examined by optical profilometry. A radial change in mechanical properties was observed. The local elastic modulus (Young's modulus) and hardness for the edge and core regions are reported. These mechanical properties were investigated with respect to deposition parameters and corresponding fiber microstructure.

PACS 81.15.Fg; 81.05.Uw; 46.55.+d

## 1 Introduction

The interest in the laser-assisted chemical vapor deposition (LCVD) process is explained by its ability to produce a variety of three-dimensional microscale deposits directly from the gas phase. The flexibility in product nature and shape [1], the process control recently achieved by various feedback systems [2, 3], and the high growth rates compared to other CVD techniques [1] make it an attractive processing tool.

Carbon has been used to produce rods [4], lines [5], trussed structures [6], and microsolenoids [7]. Carbon can be deposited from cheap, easily available, and stable precursor gases. A variety of solid-state arrangements (from amorphous carbon to graphite) having different thermal, electrical, and mechanical properties can be obtained by changing the process parameters.

With respect to mechanical applications, the interest in carbon lies in its high strength-to-weight ratio. Mechanical testing of carbon whiskers and fibers has shown the advantage of such fibers over conventional metals. Carbon fibers have high elastic moduli between 200 GPa and 800 GPa [8]. Also, high-pressure LCVD-produced fibers have tensile

strengths approaching those of commercial intermediate-modulus fibers [1].

As far as low-pressure LCVD fibers are concerned, a recent Raman investigation has shown a radial change in microstructure [9]. To the authors' knowledge, no measurement of the local mechanical properties of such fibers has been done so far. Hence, a radial analysis of the mechanical properties, achieved by nanoindentation, is presented in this paper.

Nanoindentation has been an invaluable tool in recent years to investigate the mechanical properties of amorphous carbon films (DLC, a-C) [10, 11] and various carbon-containing coatings [12, 13]. Its high spatial resolution and accepted reliability make it an easy way to investigate mechanical properties on the microscale.

The main contribution of this work is that it directly relates the mechanical properties to the process parameters that determine the characteristic microstructure of the deposit.

## 2 Experimental

### 2.1 The LCVD experiment

Cylindrical carbon microfibers were deposited on a glassy carbon substrate from ethylene at different precursor pressures and laser powers using an LCVD system. A system schematic is shown in Fig. 1. The light source used was a Coherent model Innova 90 continuous-wave argon-ion laser with a Gaussian intensity profile, operated at 514.5 nm, with a spot size of 88  $\mu\text{m}$ . Tracking of the focus with a three-axis micro-positioning system allowed steady-state growth and uniform fibers.

### 2.2 Deposition parameters

A first set of fibers was produced at an average pressure of 985 mbar with laser powers ranging from 0.2 W to 1.25 W. Another set of fibers was produced at a constant laser-power setting of 0.75 W with pressures ranging from 233 mbar to 813 mbar. These different powers and pressures produced fiber diameters of 35–135  $\mu\text{m}$ .

### 2.3 Sample preparation

The fibers were removed from the substrate, cast in acrylic resin, and then polished perpendicularly to the growth axis to show the cross section. The polishing was first done

✉ Fax: +1-514/340-3246, E-mail: remi.longtin@polymtl.ca

\*Current address: Freeform Fabrication Laboratories, Department of Mechanical Engineering, École Polytechnique de Montréal, Box 6079, Station A, Montréal, PQ H3C 3A7, Canada

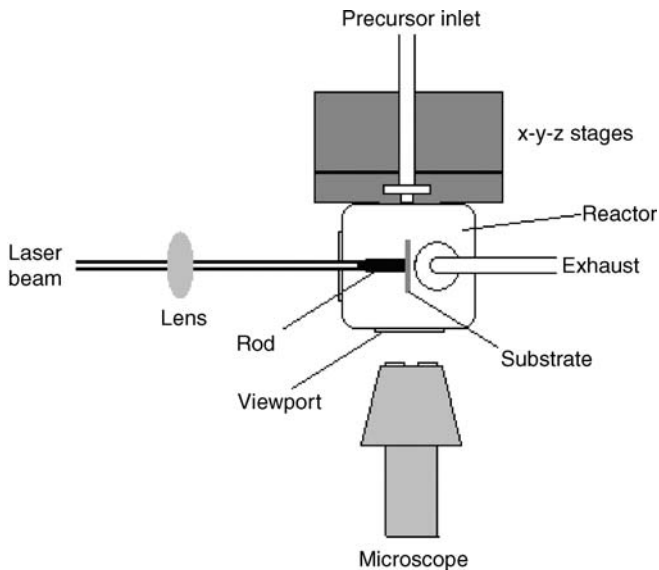


**FIGURE 1** LCVD system schematic

with silicon carbide papers and then with diamond particles down to  $1\ \mu\text{m}$  in size. The samples were cleaned with ethanol and placed in an ultrasonic bath. A WYKO optical profilometer was used to examine the cross sections and to assess the fiber diameters. All the samples were adequate for nanoindentation with a maximum surface roughness of  $1\text{--}4\ \mu\text{m}$ , which is below the indenter's  $10\text{-}\mu\text{m}$  approach-height limit. Also, a measurement of a single fiber's surface was done. It was secured on its side in acrylic resin and indented along the growth axis. Figure 2 shows a typical fiber cross-sectional profile after polishing.

## 2.4 Nanoindentation

A Berkovich diamond tip was used and the indents, approximately  $150\ \text{nm}$  deep, were placed  $2\ \mu\text{m}$  apart in a straight line across the center of the fiber. The indenting was started  $1\ \mu\text{m}$  from the fiber's surface and was stopped prior to the opposite edge to avoid indenting past the fiber.

The measurements were conducted using a XP Nanoindenter (Nano Instruments, Oak Ridge, TN, USA). The hardness ( $H$ ) and elasticity modulus ( $E$ ) were calculated from the load–displacement curves according to the Oliver and Pharr procedure [14]. The equipment was calibrated between every

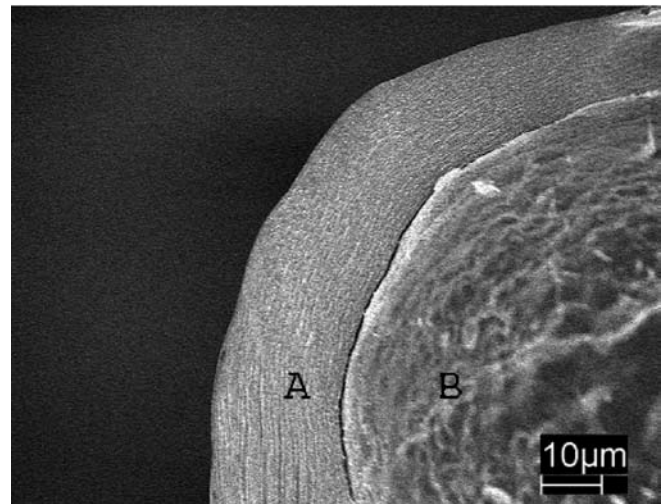


**FIGURE 3** Scanning electron micrograph of the internal structure of a fiber, exposed by cleaving, showing the interface between A the edge region and B the core region

measurement by indentation of a fused-silica reference sample. An uncertainty of 5% in the measurements was found based on the standard deviation of the measured values for the fused-silica reference and for a glassy carbon test sample.

## 2.5 Microstructure

The fibers are graphitic in nature [9]. A Raman spectroscopy analysis [15] has shown that there exist three distinct fiber regions. The exterior surface of the fiber, approximately  $1\text{-}\mu\text{m}$  thick, is made of amorphous carbon. The edge region is layered nanocrystalline graphite. The core region is well-crystallized graphite with crystal sizes as high as  $80\ \text{nm}$ . This radial change in microstructure is induced by the laser's Gaussian power distribution [9]. There is a clear interface between the edge and core regions. The different regions are shown in Fig. 3.

## 3 Results and discussion

### 3.1 Radial change in mechanical properties

For all samples indented, the local elastic modulus value decreases, from edge to center, as the structure changes from nanocrystalline to near-microcrystalline graphite. A symmetrical behavior is observed. Figure 4 shows

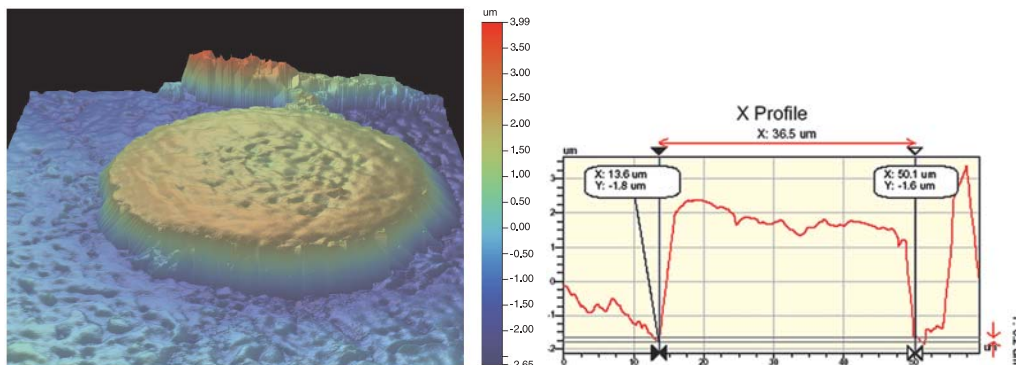


**FIGURE 2** Left: 3D plot of the embedded fiber's cross section. Right: 2D interferometer profile

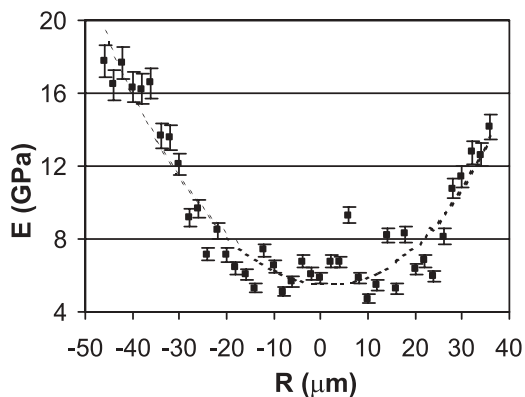


FIGURE 4 Elastic modulus vs. fiber radius. Fiber deposited at 985 mbar and 1.0 W

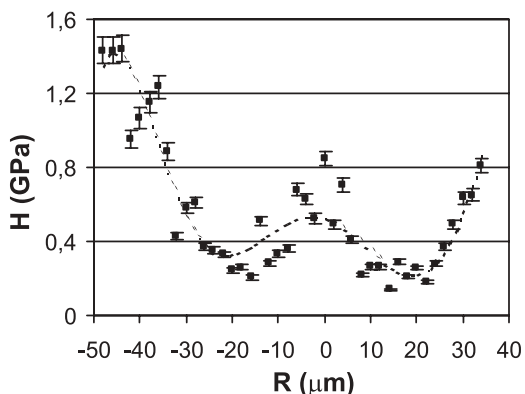


FIGURE 5 Hardness vs. fiber radius. Fiber deposited at 985 mbar and 1.0 W

the typical trend of elastic modulus as a function of radius. A fourth-degree polynomial was fitted to emphasize the trend.

The trend in modulus is a direct consequence of the radial change in microstructure. The elastic modulus is an indicator of bond structure and strength. In the case of solid-state carbon, preferred-oriented crystals (graphite) have lower elastic modulus than more randomly ordered crystals (amorphous carbon). Although graphite has strong planar carbon-carbon bonding, which maintains a high degree of order and gives it high in-plane strength, a weaker  $\pi$ -bond linking the individual sheets reduces the overall strength of the structure.

For LCVD fibers, the surface and the edge regions deposit at lower temperatures and are less graphitized. This explains why they have higher values of elastic modulus. Lower values of modulus are found at the center where maximum graphitization occurs.

The observed trend for hardness is different. The hardness decreases going from the edge to the interface of the core region, where it then increases gradually until it attains a maximum at the center of the fiber. This can be seen in Fig. 5.

This behavior is due to a shift in deformation mode in the core region. In the edge region, the material is deformed both elastically and plastically giving rise to accurate values of hardness and elastic modulus. Due to the graphitic nature of the core region, the material is only 'flexing' under the load with very minor plastic deformation. The hardness values at the center are too high and unreliable since the load was in-

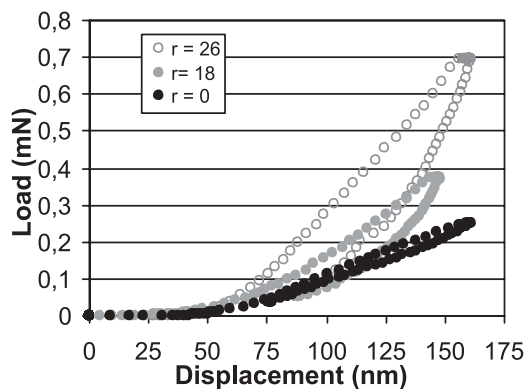


FIGURE 6 Evolution of the load-displacement curves with radius

sufficient for plastic deformation to occur. In this case, the maximum load required to reach the target depth represents the force required to both deform the planes and to penetrate the material. For this reason, only the maximum and minimum values of hardness in the edge region are reported in this work. These local maximum and minimum values are used to show a trend rather than being absolute values of hardness.

The load-displacement curves presented in Fig. 6 illustrate the radial change in deformation mechanism. From the curves, as the radius decreases the load required for the target displacement decreases. This implies a softer material at the center. Also, the very elastic response of the core region is seen from the lack of significant hysteresis between the loading and unloading curves. Nevertheless, there is some form of plastic deformation occurring since a non-zero area is observed between the curves.

### 3.2 Parameter dependence of mechanical properties

In the LCVD process, as we increase the laser power at a constant pressure we increase the temperature and the growth rate [16, 17]. At a constant laser power, increasing the reactor pressure increases the linear growth rate. An increase in temperature increases graphitization since a higher crystalline order needs more energy to be formed. An increase in growth rate hinders graphitization since it reduces the residence time of the focal point at a specific area of the fiber. The effects of pressure and laser power on the local mechanical properties are now presented since they affect the microstructure of the deposit, hence its local mechanical properties.

**3.2.1 Variable pressure and constant power:** Four different pressures were used to deposit fibers at a constant power. Figure 7 shows the elastic modulus at the edge ( $1 \mu\text{m}$  from the surface) and at the center of the fibers as a function of pressure. Figure 8 shows the maximum and the minimum values of hardness in the edge region as a function of pressure. The maximum value reported is taken  $1 \mu\text{m}$  from the surface and the minimum is taken at the interface of the core region.

The elastic modulus and the hardness increase with pressure in every region of the fiber. The mechanical properties increase since higher linear growth rates, brought about by higher pressures, increase amorphization.

The elastic modulus at the center and at the edge doubles in value with a three-fold increase in pressure. With respect to hardness, the maximum value slightly increases with pressure whereas the minimum value increases five-fold.

*Elastic modulus and crystalline order.* Raman studies [15] of samples grown using the same experimental parameters showed that the crystal size decreases with pressure. The crystal size was estimated from the  $I_D/I_G$  ratio according to the Tuinstra–Koenig equation [18]:

$$\frac{I(D)}{I(G)} = \frac{C(\lambda)}{L_a} \quad \text{with } C(514.5) \approx 44 \text{ \AA}, \quad (1)$$

where  $I(D)$  and  $I(G)$  are the  $D$  and  $G$  peak intensities,  $L_a$  the crystal basal plane length, and  $C$  a function of the laser wavelength.

Plotting the elasticity modulus against crystal size as seen in Fig. 9 shows how the mechanical properties improve with decreasing graphitization.

**3.2.2 Variable power and constant pressure.** A total of six different laser-power settings were used with a constant pressure. Figure 10 shows the elastic modulus at the center and at the edge as a function of laser power. Figure 11 shows the hardness in the edge region with respect to laser power. Again, the

maximum value reported is taken 1  $\mu\text{m}$  from the surface and the minimum is taken at the interface of the core region.

From Fig. 10, it can be seen that the center’s modulus decreases with increasing laser power between 0.2 W and 0.5 W, after which it increases again. At the edge, the values attain a minimum at 0.3 W instead of at 0.5 W before increasing again with laser power. This is due to an indent-position misalignment for the 0.3-W sample. Indenting was started further away from the fiber’s surface, hence making the modulus value at the edge lower than it should be.

As seen in Fig. 11, in the edge region there is a decrease in hardness between 0.2 W and 0.5 W. Above 0.5 W, it in-

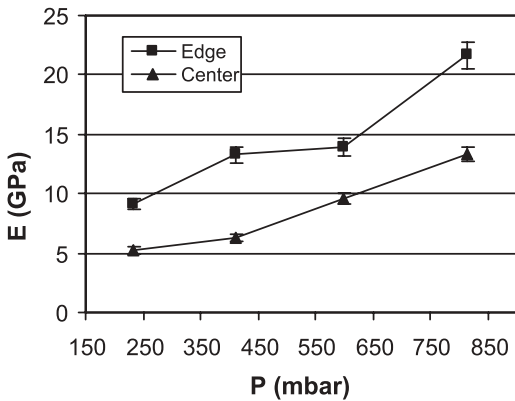


FIGURE 7 Elastic modulus at the center and at the edge as a function of pressure

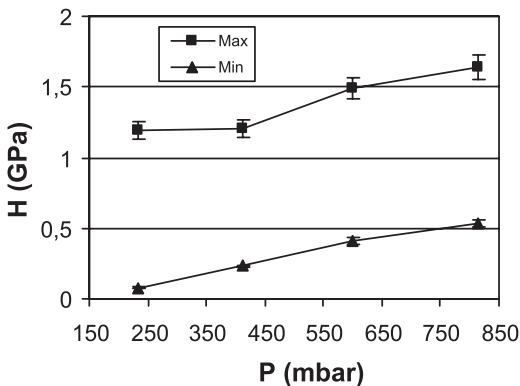


FIGURE 8 Extreme values of hardness in the edge region as a function of pressure

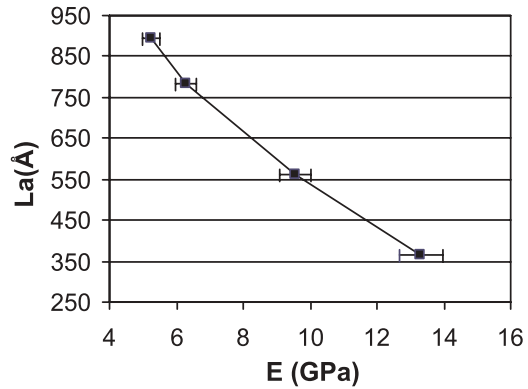


FIGURE 9 Crystal size vs. elastic modulus at the center

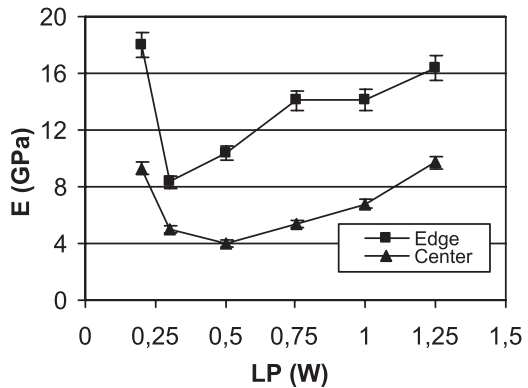


FIGURE 10 Elastic modulus at the edge and at the center as a function of laser power

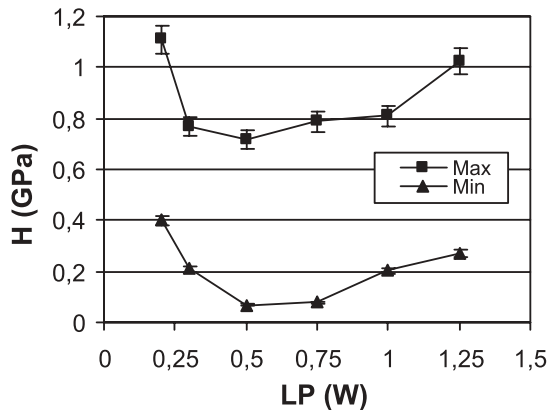


FIGURE 11 Extreme values of hardness in the edge region as a function of laser power

creases with increasing power. The trends in elasticity and hardness are explained by the different degrees of graphitization achieved in the samples [15].

Therefore, the local mechanical properties result from laser-power dependence and change according to the degree of graphitization reached during deposition.

### 3.3 Fiber surface

A Raman analysis showed that the amorphous fiber surface was very similar for all samples [15]. Indenting of a single fiber's surface produced average elastic modulus and hardness values of 20 GPa and 2.8 GPa respectively.

### 3.4 Comparison of mechanical properties

Other carbon specimens were indented for comparison. A plate of highly oriented pyrolytic graphite (HOPG) had an elastic modulus and hardness of 5 GPa and 0.2 GPa respectively. The fiber's center region modulus and hardness approached these values. A V20-grade glassy carbon plate had modulus and hardness values of 25 GPa and 3.7 GPa respectively. The maximum modulus and hardness in the edge region and at the surface approached these values.

## 4 Conclusion

Polycrystalline graphite microfibers produced by LCVD at atmospheric and sub-atmospheric pressures have low hardness and elastic modulus. For the nanocrystalline edge region, local elastic modulus values of 9 to 22 GPa and hardness values of 0.1 to 1.6 GPa were measured. For the core, local elastic modulus values of 5 to 13 GPa were obtained. Hardness measurements at the center were inconclusive. The local mechanical properties are directly related to the microstructure induced by the Gaussian laser intensity distribution. The elastic modulus decreases, from edge to center, as the structure changes radially from nanocrystalline to near-microcrystalline graphite ( $L_a < 100$  nm). Varying the deposition parameters showed that the local elastic modulus and hardness increased with amorphization. This is achieved

by increasing the pressure and increasing the laser power above a specific turning point. The LP-LCVD (Low Pressure Laser Chemical Vapor Deposition) fibers have poor mechanical properties when compared to other forms of carbon. The fibers are expected to be structurally weak due to their layered graphitic nature [19]. Even so, the material's elasticity could prove useful in certain micromechanical applications, especially in the design of low-load highly sensitive microcoils.

## REFERENCES

- 1 F.T. Wallenberger, P.C. Nordine, M. Boman: *Comput. Sci. Technol.* **51**, 193 (1994)
- 2 J.L. Maxwell, J. Pegna, D.V. Messia: *Appl. Phys. A* **67**, 323 (1998)
- 3 D. Jean, C. Duty, R. Johnson, S. Bondi, W.J. Lackey: *Carbon* **40**, 1435 (2002)
- 4 D. Bäuerle: *Laser Processing and Chemistry*, 2nd edn. (Springer, Berlin 1996)
- 5 H. Westberg, M. Boman, A.-S. Norekrans, J.-O. Carlsson: *Thin Solid Films* **215**, 126 (1992)
- 6 J. Pegna, D. Messia, W.H. Lee: in *Solid Freeform Fabrication Symp. 1997*, p. 49
- 7 K. Williams, J. Maxwell, K. Larsson, M. Boman: in *Proc. 12th IEEE Int. Conf. Micro Electro Mechanical Systems (MEMS), Orlando, FL, USA, 1999*, pp. 232–237
- 8 M.S. Dresselhaus, G. Dresselhaus, K. Sugihara, I.-L. Spain, H.A. Goldberg: *Graphite Fibers and Filaments* (Springer Ser. Mater. Sci.) (Springer, Berlin 1988) p. 122
- 9 C. Fauteux, J. Pegna: *Appl. Phys. A* (2003), DOI 10.1007/s00339-003-2084-x
- 10 E. Martínez, J. L. Andújar, M.C. Polo, J. Esteve, J. Robertson, W.I. Milne: *Diamond Relat. Mater.* **10**, 145 (2001)
- 11 M. Lindstam, O. Wänstrand, M. Boman, K. Piglmayer: *Surf. Coat. Technol.* **138**, 264 (2001)
- 12 V.L. Solozhenko, S.N. Dub, N.V. Novikov: *Diamond Relat. Mater.* **10**, 2228 (2001)
- 13 O. Takai, N. Tajima, H. Saze, H. Sugimura: *Surf. Coat. Technol.* **142–144**, 719 (2001)
- 14 W.C. Oliver, G.M. Pharr: *MRS Bull.* **7**, 1564 (1992)
- 15 C. Fauteux, R. Longtin, J. Pegna, M. Boman: *J. Appl. Phys.* (accepted November 26th, 2003, in press)
- 16 G. Leyendecker, D. Bäuerle, P. Geitner, H. Lydtin: *Appl. Phys. Lett.* **39**, 921 (1981)
- 17 G. Leyendecker, H. Noll, D. Bäuerle, P. Geitner, H. Lydtin: *J. Electrochem. Soc.* **130**, 157 (1983)
- 18 F. Tuinstra, J.L. Koenig: *J. Chem. Phys.* **53**, 1126 (1970)
- 19 L.S. Nelson, N.L. Richardson: *Mater. Res. Bull.* **7**, 975 (1972)